Two-Dimensional Nanocomposites: Alternating Inorganic-Organic Polymer Layers in Zirconium Phosphate

Yi Ding,† Deborah J. Jones,* Pedro Maireles-Torres, and Jacques Rozière

Laboratoire des Agrégats Moléculaires et Matériaux Inorganiques URA CNRS 79, Université Montpellier 2, Place Eugène Bataillon, 34095 Montpellier cedex 5, France

Received October 14, 1994. Revised Manuscript Received January 2, 1995[⊗]

α,ω-Amino acids have been intercalated into α-zirconium phosphate (α-ZrP) to give expanded phases enclosing an amino acid monolayer. The ϵ-aminocaproic acid-α-ZrP hybrid is a particularly useful intermediate, since it permits ion-exchange reactions at pH values a low as 2.6 and so provides access to a new area of zirconium phosphate intercalation chemistry. When used as a precursor, both linear (e.g., acrylamide) and cyclic (e.g., 2-pyrrolidinone, δ-valerolactam, ϵ-caprolactam) amides as well as macromolecular polyamides such as protamine, gelatin, and lysozyme can be inserted. Zirconium phosphate platelets are clearly seen in scanning electron microscopy, and there is no evidence for surface sorption of the biopolymers. The ϵ-aminocaproic acid-α-ZrP intercalation compound is itself a precursor to a polymer-inorganic nanocomposite since the in situ polymerization to nylon-6, identified by infrared and ^{13}C NMR spectroscopies both in its as-synthesized occluded environment and ex situ following destruction of the phosphate matrix and recuperation of the polymer released. These surface-modified zirconium phosphates are organic-inorganic hybrids and are materials of potential use as protonic conductors or as intermediates in the synthesis of novel porous solids.

Introduction

Zirconium hydrogen phosphate has been much studied in the past for its ion-exchange behavior[1] and is currently inciting renewed interest as a host matrix for the preparation of nanocomposite solids via the intercalation of organic,[2-6] organometallic,[7-9] or inorganic oligomeric species,[10-13] largely due to its high thermal stability relative to that of its clay counterparts. The modification of the interlayer region of two-dimensional substrates by intercalation/formation of organic polymers to form nanocomposite solids composed of alternating inorganic and organic layers has received significant attention over recent years.[3-6,14-20] The resulting physical, mechanical, or thermal properties of the composite solid are, in many cases, a direct consequence of the effect of polymer confinement in an organized medium.[18,19] As one of a number of examples, greatly improved tensile strengths, and heat distortion temperatures have been reported for clay-dispersed nylon-6,[21] and aminoundecanoic acid intercalated montmorillonite has been used as a precursor for a coupled clay delamination-epoxyresin polymerization process.[22] Imposed stereospecificity, electrical conductivity, nonlinear optical properties etc. have also been observed, exceeding the expected effect of mechanical or thermal reinforcement.

In a similar context, the development of improved micro- and mesoporous materials derived by pillaring layered solids other than clays may be considered to depend, to certain extent, on advances in convergent areas, among which may be cited the availability of novel precursor solids capable of, for example, ion

† Present address: School of Chemical Engineering, Georgia Institute of Technology, GA 30332-0100.

[⊗] Abstract published in *Advance ACS Abstracts,* February 1, 1995.

(1) (a) Alberti, G. *Inorganic Ion-Exchange Materials*; Clearfield, A., Ed.; CRC Press: Boca Raton, FL, 1982. (b) Constantino, U. *Ibid.*; pp 111-132.

(2) Herzog-Cance, M. H.; Jones, D. J.; El Mejjad, R.; Rozière, J.; Tomkinson, J. *J. Chem. Soc., Faraday Trans.* **1992**, 88, 2275.

(3) Jones, D. J.; El Mejjad, R.; Rozière, J. *Supramolecular Architecture in Thin Films and Solids*; ACS Symp. Ser.; Bein, T. Ed.; 1993.

(4) Pillion, J. E.; Thompson, M. E. *Chem. Mater.* **1991**, *3*, 777.

(5) Chao, K. J.; Chang, T. C.; Ho, S. Y. *J. Mater. Chem.* **1993**, *3*, 427.

(6) Costantino, U.; Marmottini, F. *Mater. Chem. Phys.* **1993**, *35*, 193.

(7) Rozière, J.; Jones, D. J.; Cassagneau, T. *J. Mater. Chem.* **1991**, *1*, 1081.

(8) Jones, D. J.; Cassagneau, T.; Rozière, J. *Multifunctional Mesoporous Inorganic Solids*; Sequeira, C. A. C., Hudson, M. J., Eds.; NATO ASI, **1993**, *400*, 289; Kluwer Academic: Dordrecht.

(9) Cassagneau, T.; Jones, D. J.; Rozière, J. *J. Phys. Chem.* **1993**, *97*, 8678.

(10) Maireles-Torres, P.; Olivera-Pastor, P.; Rodriguez-Castellon, E.; Jimenez-Lopez, A.; Alagna, L.; Tomlinson, A. A. G. *J. Mater. Chem.* **1991**, *1*, 319.

(11) Maireles-Torres, P.; Olivera-Pastor, P.; Rodriguez-Castellon, E.; Jimenez-Lopez, A.; Tomlinson, A. A. G. *J. Mater. Chem.* **1991**, *1*, 739.

(12) Maireles-Torres, P.; Olivera-Pastor, P.; Rodriguez-Castellon, E.; Jimenez-Lopez, A.; Tomlinson, A. A. G. *J. Solid State Chem.* **1991**, *94*, 368.

(13) Clearfield, A.; Roberts, B. D. *Inorg. Chem.* **1988**, *27*, 3237.

(14) Ruiz-Hitzky, E.; Aranda, P. *Adv. Mater.* **1990**, *2*, 545.

(15) (a) Kanatzidis, M. G.; Marcy, H. O.; Wu, C. G.; DeGroot, D. C.; Kannewurf, C. R. *Adv. Mater.* **1990**, *2*, 364 (b) Kanatzidis, M. G.; Wu, C. G.; Marcy, H. O.; DeGroot, D. C.; Kannewurf, C. R. *Chem. Mater.* **1990**, *2*, 222.

(16) Cao, G.; Mallouk, T. E. *J. Solid State Chem.* **1991**, *94*, 59.

(17) Mehotra, V.; Giannelis, E. P. *Solid State Ionics* **1992**, *51*, 115.

(18) Ruiz-Hitzky, E. *Adv. Mater.* **1993**, *5*, 334.

(19) Messersmith, P. B.; Giannelis, E. P. *Chem. Mater.* **1993**, *5*, 1064.

(20) Vaia, R. A.; Ishii, H.; Giannelis, E. P. *Chem. Mater.* **1993**, *5*, 1694.

(21) (a) Okada, A.; Kawasumi, M.; Usuki, A.; Kojima, Y.; Kurauchi, T.; Kumigaito, O. *Mater. Res. Soc. Symp. Proc.* **1990**, *171*, 45. (b) Okada, A.; Kawasumi, M.; Kurauchi, T.; Kamigaito, O. *Polym. Prepr.* **1987**, *28*, 447.

(22) Wang, M. S.; Pinnavaia, T. J. *Chem. Mater.* **1994**, *6*, 468.

0897-4756/95/2807-0562$09.00/0

exchanging at low pH values, or on the development of new routes designed to overcome the drawback represented by high layer charge densities. One such approach currently under study in this laboratory concerns the modification/stabilization of metal sols containing the inorganic species serving as pillar precursors using organic oligomers.

Most generally, inorganic solid–polymer nanocomposites have been prepared in situ by adsorption of an appropriate monomer followed by polymerization, which may be induced thermally or chemically, often via a redox process. Direct intercalation of polymers from solution may be considered as a less generalizable approach, since the possibility of insertion depends on a number of factors, including the charge density on the layers and pK value of the polymer. A novel direction has been indicated recently by Giannelis et al., who achieved direct insertion into a surface modified mica-type silicate from polymer melts.[20]

These various aspects provided the impetus for the research reported below, in which the preparation of a number of organozirconium phosphate composites is described. The α,ω-amino acid intercalation compounds are temporally and chemically stable, but their principal interest lies in their use as precursors for intercalation processes at pH <3.5, which proceed otherwise only partially, if at all, so allowing the insertion of not only small organic molecules such as acrylamide and lactams (2-pyrrolidinone, δ-valerolactam, ϵ-caprolactam) but also biologically active macromolecules such as protamine and gelatin, which are known to stabilize metal sols, and lysozyme, so demonstrating the possibility of immobilizing enzymes in α-ZrP. They are precursors also for polymerization reactions in situ, with formation, for example, of the first nylon-6 zirconium phosphate hybrid.

Experimental Section

Materials. Acrylamide, 2-pyrrolidinone, δ-valerolactam, ϵ-caprolactam, and ϵ-aminocaproic acid were Aldrich products. The proteins used were obtained from Sigma: lysozyme (from hen egg white, $M_r \sim 14\,600$), protamine free base (grade IV, from salmon), gelatin (from porcine skin). α-zirconium phosphate [$Zr(HPO_4)_2 \cdot H_2O$] was prepared according to the method described by Alberti and Torracca.[23]

Synthesis of ϵ-Aminocaproic Acid–α-ZrP (AMC-α-ZrP). The ϵ-aminocaproic acid–α-ZrP intercalation compound was prepared by contacting α-zirconium phosphate (8 g) with an aqueous solution of ϵ-aminocaproic acid (0.25 M, 300 cm^3), for 7 days under reflux conditions. After cooling to room temperature, the suspension was centrifuged and the solid recovered well washed with distilled water and air-dried.

Synthesis of Amide–α-Zirconium Phosphate Intercalates. To a 1% (w/v) aqueous suspension of AMC-α-ZrP was added an excess of monomeric amide, either as a neat liquid (2-pyrrolidinone, δ-valerolactam) or as an aqueous solution for acrylamide and caprolactam. The pH was adjusted to 3.0–3.2 for the three former, pH 4.0 for caprolactam, by using 0.1 M HCl. This pH range facilitates the exchange of the pre-intercalated aminocaproic acid and avoids the regeneration, at a lower pH, of pure α-zirconium phosphate with a basal spacing too low to allow amide intercalation. After 6 days of contact time at room temperature, the solids were separated by centrifugation, washed thoroughly with distilled water, and air-dried.

Synthesis of Macromolecular Polyamide–α-Zirconium Phosphate Intercalates. An aqueous solution of the proteins gelatin, lysozyme, and protamine (1 g/250 cm^3) was added to an aqueous suspension of AMC–α-ZrP (1.0 g/50 cm^3). For gelatin and lysozyme, the initial pH was adjusted to 3.0 and 2.6, respectively, whereas for protamine, intercalation can be carried out at the natural pH of the solution. The contact time necessary for complete displacement of AMC from zirconium phosphate was short for gelatin (6 h) and longer for protamine (8 days) and lysozyme (17 days), indicating clear differences in their intercalation kinetics. After this time, intercalates were separated by centrifugation, washed with hot distilled water to eliminate externally adsorbed proteins, and air-dried.

Formation of Interlayer Nylon-6 from AMC–α-ZrP. Synthesis of poly(aminocaproic acid), "nylon-6", in the interlayer region was performed by heating AMC–α-ZrP at 260 °C under a N_2 atmosphere for 1 h, with a heating rate of 1 °C min^{-1}. Extraction of nylon-6 was performed by means of hydrofluoric acid (20%) treatment of the nanocomposite, which destroys the inorganic matrix and leaves the released polymer as a whitish lump which was water-washed prior to spectroscopic analysis.

Characterization. X-ray diffraction (XRD) was performed on an automated Philips powder diffractometer allowing multiple scanning, using Cu Kα radiation. TGA-DTA measurements were carried out under air and nitrogen using a Stanton Redcroft STA 781 instrument (calcined Al_2O_3 reference, 3 °C min^{-1} heating rate). Infrared (IR) spectra between 400 and 4000 cm^{-1} were recorded on KBr disks, using a FT Bomem DA8 spectrometer. ^{13}C CP-MAS NMR spectra of the ϵ-aminocaproic acid–ZrP intercalate, the corresponding in situ polymerized phase, and of the polymer extracted by degradation of the host matrix, as well as of bulk aminocaproic acid and of nylon-6 formed ex situ for comparison, were obtained using a Bruker AM300 instrument operating at 75.5 MHz. Chemical shifts were determined with respect to an external standard of liquid tetramethylsilane.

An Erba Science 1108 instrument provided C, H, and N analyses. Scanning electron micrographs of the AMC–α-ZrP precursor and of the biopolymer–ZrP intercalates were obtained using LEICA Cambridge Model S360 instrument.

Table 1. Isoelectric Points of Some L-Amino Acids

L-amino acid	isoelectric point
asparagine	5.4
α-alanine	6.0
histidine	7.5
lysine	9.7
arginine	10.7

Results and Discussion

Intercalation of α,ω-Amino Acids in α-Zirconium Phosphate. Some years ago, Kijima reported the relative ready insertion of biologically active α-L-amino acids into the α and γ ($ZrPO_4 \cdot H_2PO_4 \cdot 2H_2O$) forms of zirconium phosphate. For α-ZrP, only basic amino acids (histidine, lysine, and arginine) could be intercalated, whereas asparagine and alanine were surface adsorbed.[24,25] The ease of intercalation of α-amino acids into α-ZrP can therefore be related to the isoelectric point of the amino acids (Table 1), with a cutoff point between 6 and 8. The three α,ω-amino acids investigated here have isoelectric points in this range.

The adsorption isotherm of β-alanine ($H_2N(CH_2)_3CO_2H$, isoelectric point 6.9) by α-ZrP at 25 °C has the form shown in Figure 1. Depending on the substrate: intercalant ratio, two different layered phases are observed, which have interlayer distances (determined

(23) Alberti, G.; Torracca, E. *J. Inorg. Nucl. Chem.* **1968**, *30*, 317.

(24) (a) Kijima, T.; Sekikawa, Y.; Ueno, S. *J. Inorg. Nucl. Chem.* **1981**, *43*, 849. (b) Kijima, T.; Ueno, S.; Goto, M. *J. Chem. Soc., Dalton Trans.* **1982**, 2499.

(25) Kijima, T.; Ueno, S. *J. Chem. Soc., Dalton Trans.* **1986**, 61.

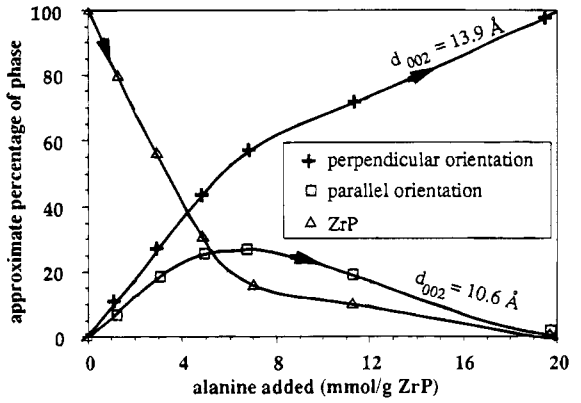

Figure 1. Adsorption isotherm of β-alanine by α-ZrP at room temperature.

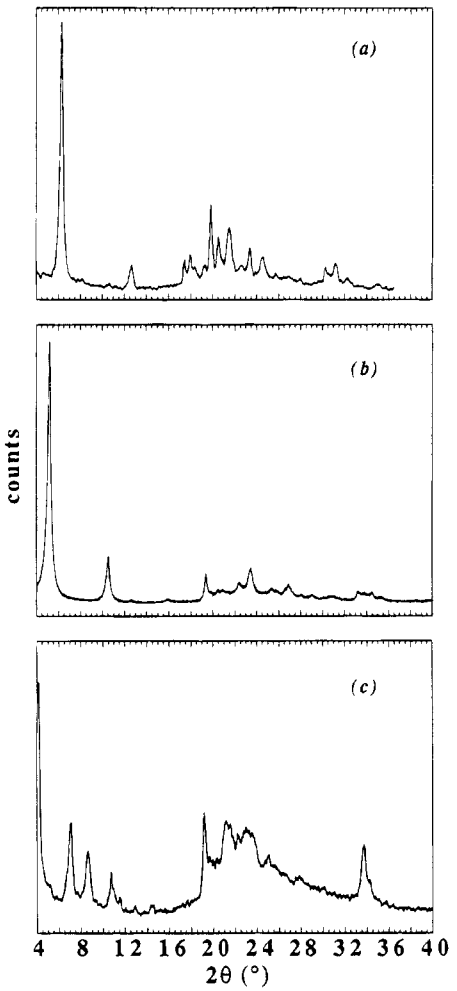

Figure 2. Powder X-ray diffraction patterns of intercalates: (a) β-alanine–ZrP; (b) ϵ-aminocaproic acid–ZrP; (c) amino-undecanoic acid–ZrP.

from the d_{002} reflection) of 10.6 and 13.9 Å. The former basal spacing is characteristic of intercalated aliphatic molecules adopting an orientation parallel to the ZrP layers.[26] Only the latter of the two intercalates above can ultimately be obtained as a single phase, Figure 2a, indicating that the former is an intermediate in the insertion process produced at low concentrations of alanine in solution. The stoichiometry derived from C, H, N analysis of the 13.9 Å phase is $Zr(PO_4)_{0.8}$-$(HPO_4)_{1.2}[H_3N(CH_2)_2CO_2H]_{0.8}\cdot H_2O$, and it is concluded that, even at high concentrations, uptake is limited to a monolayer. In this respect, similarity is found with the family of diamine intercalates of α-zirconium phosphate, where a single layer of molecules suffices to saturate the active sites–POH on the host substrate.[27] For α,ω-amino acids, as for α,ω-diamines, hydrogen-bonding interactions are expected between the end-group functions and the phosphate and hydrogen phosphate groups in the layers above and below.

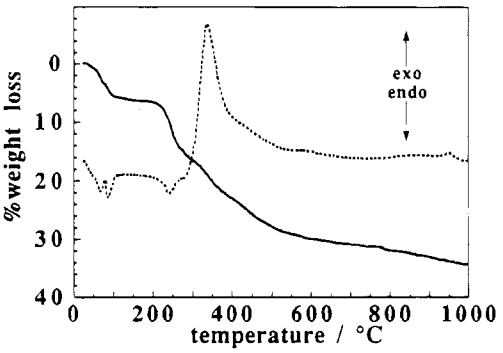

Figure 3. Thermogravimetric-differential thermal analysis of ϵ-aminocaproic acid–ZrP performed in air.

The ϵ-aminocaproic acid-ZrP system contains three distinct phases. The first, of interlayer spacing 16.3 Å (Figure 2b), has the composition α-$Zr(HPO_4)_2$–$(H_2N(CH_2)_5CO_2H)_{0.80}\cdot 1.5H_2O$, and is produced by refluxing aqueous ϵ-aminocaproic acid (isoelectric point 7.6) solutions with α-ZrP. The second is a dehydrated phase of basal spacing 15.2 Å. On standing in air, this phase partially rehydrates without altering the interlayer spacing. The van der Waals length of the ϵ-aminocaproic acid molecule has been estimated as 10 Å (thickness ca. 4 Å),[28] and the observed expansion is therefore more consistent with incorporation of a single layer of guest amino acid, oriented off-perpendicular with respect to the phosphate sheets, than with a parallel-oriented bilayer. The tilt angle in the dehydrated phase can be calculated as approximately 59°. Interaction of the two functional head and tail groups with the zirconium phosphate layers above and below is expected, as in the case of β-alanine.

Thermogravimetric analysis of AMC–α-ZrP (Figure 3) shows three well-defined steps. Elimination of water is observed below 120 °C (weight loss ca. 6.5%) associated, in the DTA curve, with two endothermic effects centered at 69 and 88 °C. The TGA plateau at 120 °C is followed by a weight loss of 11% between 120 and 250 °C due to partial expulsion of ϵ-aminocaproic acid from the interlayer region.

Evidence for rearrangement of the remaining monomeric species is provided by DTA, where an endothermic effect is observable at 242 °C. XRD analysis of the compound present between these temperatures provides evidence for a third aminocaproic acid-ZrP phase, the interlayer distance of which, 10.6 Å, is consistent with an orientation of the monomer molecules parallel to the phosphate layers. The stoichiometry of this phase corresponds to $ZrP(AMC)_{0.5}$, and a schematic represen-

(26) Clearfield, A.; Tindwa, R. M. *J. Inorg. Nucl. Chem.* **1979**, *41*, 871.

(27) Casciola, M.; Costantino, U.; DiCroce, L.; Marmottini, F. *J. Inclus. Phenom.* **1988**, *6*, 291.

(28) Kato, C.; Kuroda, K.; Misawa, M. *Clays Clay Miner.* **1979**, *27*, 129.

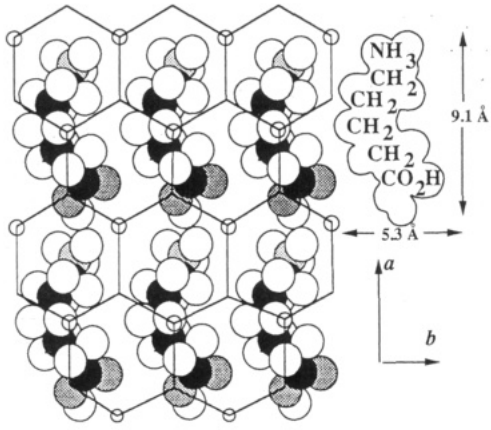

Figure 4. Schematic representation of the arrangement of ϵ-aminocaproic acid on zirconium phosphate in the layer-parallel phase.

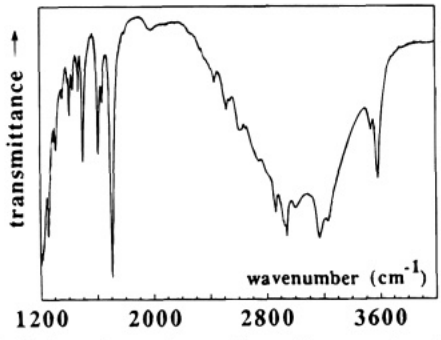

Figure 5. Infrared spectrum of ϵ-aminocaproic acid–ZrP.

tation of a projection on to the zirconium phosphate layer is shown in Figure 4. Subsequently, a second endothermic effect at 278 °C corresponds to condensation and formation of polyamide linkages to form nylon-6. At higher temperature, and when the analysis is performed in air, a strong exothermic effect, centered at 339 °C, corresponds to the combustion of the organic matter, whereas under nitrogen, several endothermic phenomena occur. The last weight loss extends up to about 900 °C, and corresponds to continued elimination of organic matter and condensation of phosphate groups to generate layered zirconium pyrophosphate, which at 950 °C presents its phase transition to the cubic form.

Confirmation of the entirely protonated nature of the aminocaproic acid molecules is provided by IR (Figure 5), where absorptions due to vibrations of the C=O and NH_3 groups are readily observed [ν(C=O), 1708; $\delta_S(NH_3)$ 1504, $\delta_{as}(NH_3)$ 1615 cm^{-1}]. Bands at 1642, 3540, and 3586 cm^{-1}, which are attributed to deformation and stretching modes of co-intercalated water, disappear after calcination at 120 °C. Absorption in the region 2400–3300 cm^{-1} is characterized by multiple fine structure on the low-wavenumber side of the band.

Attempts at direct intercalation of aminoundecanoic acid into zirconium phosphate generally produced materials in which two or more intercalated phases coexisted. An example is shown in Figure 2c, where two series of reflections can be seen in the XRD pattern, indicating interlayer distances of ca. 21 and 25 Å.

The present results may be compared with the fragmentary data available on clays. On intercalation of ϵ-aminocaproic acid into montmorillonite ion-exchanged with sodium, magnesium, calcium, copper, and cobalt, the increase in free height ranges from 4.2 to 13.2 Å, but here the presence of metal ions sometimes prevents formation of the fully protonated amino acid, which remains in its zwitterionic form.[28] Other authors report expansions of 3.6 and 6.9 Å, respectively, on insertion of aminocaproic and aminoundecanoic acids into protonated montmorillonite;[29,22] these results would seem to suggest that the significantly increased layer charge density on metal phosphates compared with clays (ca. 10 times) plays an important role in orientating the incoming guest molecules as well as increasing their uptake.

Aminocaproic Acid–α-ZrP Nanocomposite as a Precursor for Intercalation Reactions. *Intercalation of Monomeric Linear and Cyclic Amides.* Few monomeric amide molecules have been inserted in α-ZrP with, to the best of our knowledge, only the intercalation of *N*-methyl- and *N,N*-dimethylformamide[30] having been reported up to now, having basal spacings of 10.5 and 10.7 Å, respectively. Little information is available on the structural arrangements or the nature of the interaction of the amide molecules in the interlayer region in these systems.

(1) Acrylamide. Acrylamide, H_2C=CHCONH$_2$, has previously been directly intercalated into montmorillonite,[31] the polysilicic acids magadiite and kenyaite,[32] and kaolinite[33] to produce materials expanded by 5.4, 3.8, 5.8, and 4.1 Å, respectively, values close to the calculated thickness of the acrylamide molecule (3.7 Å). Recent research on the intercalation of acrylamide into α-ZrP using propanol, ethanol, and butanol expansates have produced a new phase of interlayer spacing 9.9–10.2 Å.[34] In the present study, whereas attempts at direct intercalation of acrylamide into ZrP were unsuccessful, use of the above aminocaproic acid–ZrP intercalate as a precursor provided a route to an expanded solid of phase purity ca. 95%, based on the intensities of d_{002} lines in XRD (i.e., 5% AMC–α-ZrP remains). Only attempts at pH 3.0–3.2 produced an acrylamide-predominant intercalate, the interlayer distance of which is 10.1 Å (Figure 6a), in agreement with that obtained via other expanded precursors,[34] and for which the corresponding free height of 3.5 Å is in good agreement with those given above for other layered systems.

Combined chemical and thermogravimetric (Figure 7) analyses furnish a stoichiometry of α-Zr$(HPO_4)_2$$(CH_2$-$CHCONH_2)_{0.7}$·$1.0H_2O$, compatible with a layer-parallel oriented monolayer of acrylamide molecules occluded between the ZrP layers. Confirmation is provided by IR (Figure 8), which shows absorption bands at 1708 and 1666 cm^{-1}, assigned to ν(C=O) (amide I band) and ν(C=C), respectively. The unchanged position of the carbonyl stretching frequency in the intercalate compared with bulk acrylamide suggests that host–guest interaction occurs rather through hydrogen bonding between acrylamide molecules at the amine group, and the oxygen atom of phosphate, rather than via a –POH–O=C type hydrogen bond. Thermal treatment

(29) Fukushima, Y.; Inagaki, S. *J. Inclus. Phenom.* **1987**, *5*, 473.
(30) Behrendt, D.; Beneke, K.; Lagaly, G. *Angew. Chem., Int. Ed. Engl.* **1976**, *15*, 544.
(31) Ogawa, M.; Kuroda, K.; Kato, C. *Clay Sci.* **1989**, *7*, 243.
(32) Yanagisawa, T.; Yokoyama, C.; Kuroda, K.; Kato, C. *Bull. Chem. Soc. Jpn.* **1990**, *63*, 47.
(33) Sugahara, Y.; Satokawa, S.; Kuroda, K.; Kato, C. *Clays Clay Miner.* **1990**, *38*, 137.
(34) Costantino, U., personal communication.

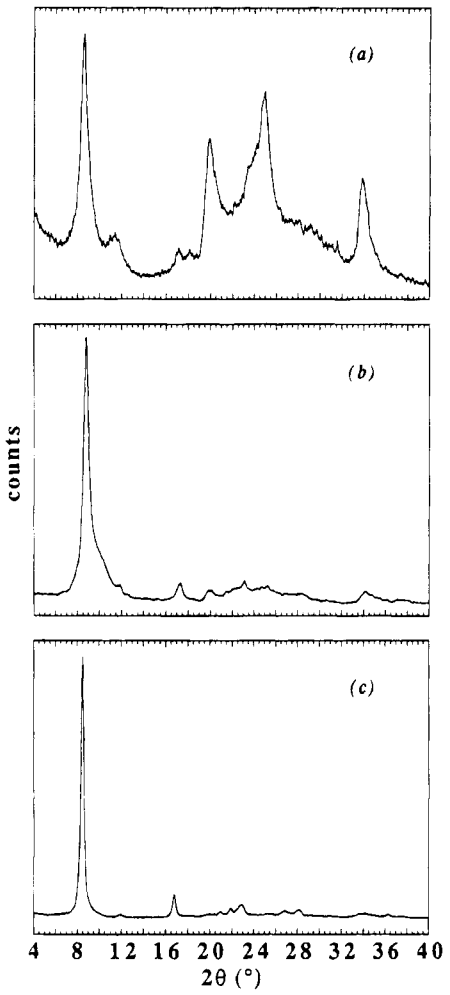

Figure 6. Powder X-ray diffraction patterns of intercalates: (a) acrylamide–ZrP; (b) 2-pyrrolidinone–ZrP; (c) δ-valerolactam–ZrP.

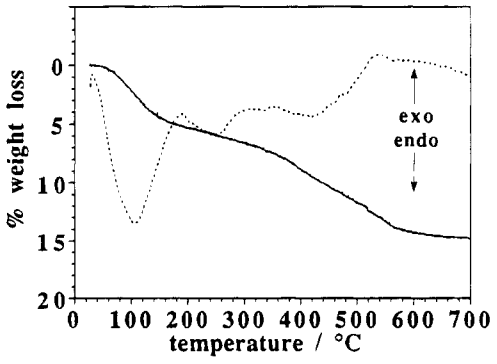

Figure 7. Thermogravimetric differential thermal analysis of ZrP–acrylamide performed under nitrogen.

under nitrogen at 240 °C produces a material of interlayer distance unchanged compared with that of starting compound but which presents an infrared spectrum consistent with polymerization in the interlayer region.[34]

(2) Intercalation of Lactams. In the present study, attempts at the direct intercalation of five- (2-pyrrolidinone) and six- (δ-valerolactam) ring lactams into α-ZrP from aqueous solution at the natural pH values of the lactam in water (4.0 and 3.2, respectively) were unsuccessful. The use of the α-ZrP–aminocaproic acid intercalate as a precursor has a striking effect on the extent of intercalation, with expanded materials obtainable after a contact time of generally 6–9 days at room temperature. The exchange reaction is nevertheless highly pH dependent, the aminocaproic acid intercalate being recovered unchanged at pH values above pH 3.5, with the range in which single-phase 2-pyrrolidinone and δ-valerolactam–α-ZrP composites can be obtained definable as 3.0–3.2. Figure 6b,c show the diffraction patterns of the intercalates, which have interlayer distances of 10.0 and 10.4 Å, respectively. The similar increase in free height in each case, 3.4–3.8 Å, infers an orientation of the rings parallel to the layers, as observed, for example, on intercalation of pyridine into α-ZrP.[35] In contrast, nonidentical increases in basal spacing were observed on intercalation of 2-pyrrolidinone and δ-valerolactam into kaolinite, and the results interpreted in terms of a probable perpendicular orientation of the organic molecules.[36]

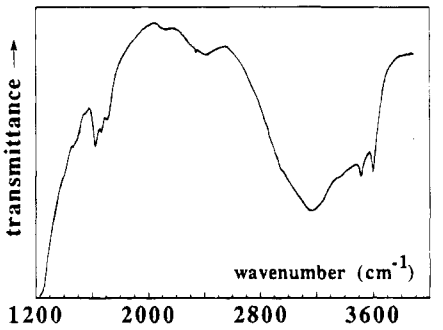

Figure 8. Infrared spectrum of the acrylamide–ZrP intercalate.

Chemical and thermogravimetric analyses indicate stoichiometries of α-$Zr(HPO_4)_2(C_4H_7NO)_{0.5}$·$1.0H_2O$ and α-$Zr(HPO_4)_2(C_5H_9NO)_{0.4}$·$1.1H_2O$, a slightly lower saturation uptake of the six-membered ring lactam compared with its five-membered congener being compatible with a parallel orientation of these species. Only 24 and 18% of active sites of the exchanger are neutralised by 2-pyrrolidinone and δ-valerolactam respectively which can, as previously reported by Yamanaka[35] for pyridine intercalation, be explained by considering the weak acid character of the lactam molecules and by assuming the presence of acidic sites of different strength in α-ZrP.

Reaction of caprolactam with AMC–ZrP produces a biphasic material of empirical formula $Zr(HPO_4)_2(C_6H_{11}NO)_{0.5}$·$1.1H_2O$. Two layered phases–$d_{002}$ = 10.2 and 15.2 Å–were systematically observed, the former, analogous to the lactam intercalates above, corresponding to intercalation of caprolactam oriented parallel to the layers, and the second to the "anhydrous" aminocaproic acid–ZrP system described above. The infrared spectrum of the biphasic system is almost identical to that of the AMC–ZrP intercalate, clearly showing the presence of carboxylic acid and protonated amine groups, and it is concluded that aminocaproic acid is derived from caprolactam by in situ acid-catalyzed ring-opening.

Intercalation of Macromolecular Polyamides. Intercalation of a number of enzymes of molecular weight as high as 240 000 (papain, lipase, peroxidase, α-amylase, glucoamylase, glucose oxidase, and catalase) into exfoliated γ-titanium phosphate has recently been

(35) Yamanaka, S.; Horibe, Y.; Tanaka, M. *J. Inorg. Nucl. Chem.* **1976**, *38*, 323.
(36) Sugahara, T.; Kitano, S.; Satokawa, S.; Kuroda, K.; Kato, C. *Bull. Chem. Soc. Jpn.* **1986**, *59*, 2607.

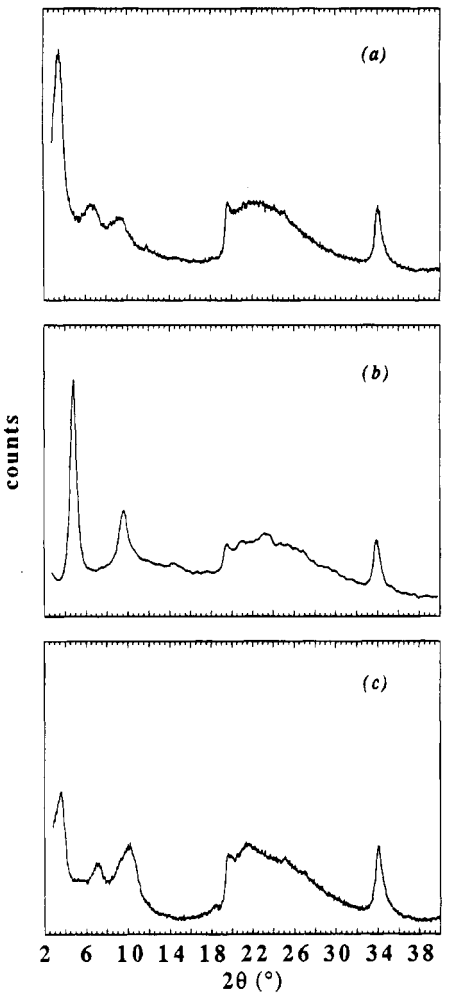

Figure 9. Powder X-ray diffraction pattern of (a) gelatin–ZrP, (b) protamine–ZrP, and (c) lysozyme–ZrP.

reported,[37] and retention of enzymatic activity has been demonstrated. While enzyme immobilization has evident applications, the possible insertion of proteins in a broader sense is important from the point of view of eventual cointercalation with inorganic pillaring ions.

Clear evidence that aminocaproic acid can be displaced by polymeric systems by adsorption from aqueous solution is provided by powder XRD (Figure 9). The three proteins were chosen to represent a class of (i) relatively low molecular weight proteins (ca. 7870) and intracrystalline arrangement of minimal complexity: protamine, (ii) a high molecular weight (ca. 60 000) fibrous protein derivative gelatin, and (iii) a medium molecular weight globular enzymatic protein (ca. 14 600): lysozyme. Once again, strict definition of pH conditions was found to be essential. Complete intercalation of gelatin and lysozyme could be achieved only at pH 3.0 and 2.6, respectively, corroborating the hypothesis that protein uptake would be expected to increase as the pH of the system falls away from the isoelectric point (pI = 4.5 for gelatin and 10.5 for lysozyme). Under these conditions, the biopolymer-zirconium phosphate composites have interlayer spacings of 18.3, 26.6, and 25.5 Å for the protamine, gelatin, and lysozyme systems, respectively.

In the case of gelatin, exchange is complete after a contact time as little as 6 h; longer reaction periods lead to the progressive appearance of broad rings in the X-ray diffraction pattern probably due to amorphization of the ZrP layers or to an increased degree of ordering of gelatin within the interlayer region. Loss of the secondary structure (hydrogen-bonding interactions between constituent amino acids) of the protein is thus implied, as on intercalation of gelatin into montmorillonite, where the presence of polypeptide chains of the β-keratin type was concluded.[38] Indeed, such "unfolding" of the protein has been considered a step essential to intercalation. If the secondary structure is effectively lost, then a simple relationship should exist between the "thickness" of the unfolded polymer chain and the observed interlayer distance, as on intercalation of monomeric species. For example, the interlayer expansion due to the presence of lysozyme molecules in zirconium phosphate can be calculated by subtracting the layer thickness of α-ZrP from the d_{002} of the composite: 25.5 Å − 6.6 Å = 18.9 Å, which is in good agreement with the dimensions of lysozyme, reported[39] as 29.7 Å × 19 Å × 18.4 Å. Similarly, protamine is expected to lead to an increase of the basal spacing of 5.8 Å; the observed expansion of 11.7 Å is thus compatible with inclusion of a protein bilayer in this case.

Table 2. Chemical Composition and Interlayer Distances of Biopolymer–α-ZrP Nanocomposites

	C/N[a]	% organic matter[b]	Δd (Å)/protein arrangement[c]
gelatin	2.8		
gelatin–ZrP	2.9	43	20.0/trilayered
protamine	1.6		
protamine–ZrP	1.6	32	11.7/bilayered
lysozyme	2.8		
lysozyme–ZrP	2.9	40	18.9/monolayered
aminocaproic acid	5.1		

[a] C:N ratio from CHN analyses. [b] Percent organic matter in the protein–ZrP composites obtained from CHN analyses. [c] Based on the known thickness of the corresponding protein chain in the bulk.

The strongest evidence that the protein molecules are not chemically degraded by the dissolution/intercalation process is provided by chemical analysis (Table 2), which indicates strictly identical carbon-to-nitrogen ratios in the bulk proteins as for those occluded between zirconium phosphate layers. Thus, for example, whereas the C/N ratio of aminocaproic acid is 5.1, that of the ZrP-gelatin composite is 2.9, to be compared with 2.8 in the bulk protein. Due to the complexity of the polymeric systems, analytical results are best expressed in terms of percent organic matter: 43% ZrP-gelatin, 32% ZrP-protamine, and 40% ZrP-lysozyme.

These data provide an additional indication that the protein lies fully in the interlayer region and is not surface-sorbed. In the lysozyme–ZrP system for example, calculation based on the percentage of organic matter and the area occupied by molecule of lysozyme [2 × (29.7 Å × 18.4 Å)], lead to a covered surface area of about 365 $m^2\ g^{-1}$ phosphate. This represents less than 40% of the total surface area of α-ZrP calculated from the unit cell parameters (a = 9.060 Å, b = 5.297 Å[40]), which is 960 $m^2\ g^{-1}$. The observed lysozyme uptake is thus below the maximum allowed for completely filling the interlayer region.

(37) Kanzaki, Y.; Abe, M. *Bull. Chem. Soc. Jpn.* **1991**, *64*, 2292.

(38) Talibudeen, O. *Trans. Faraday Soc.* **1954**, *51*, 582.

(39) Segal, J.; Dornberger-Schiff, K.; Kalaidjiev, A. *Globular Protein Molecules: their structure and dynamic properties*; Pergamon Press: New York, 1960; pp 63–64.

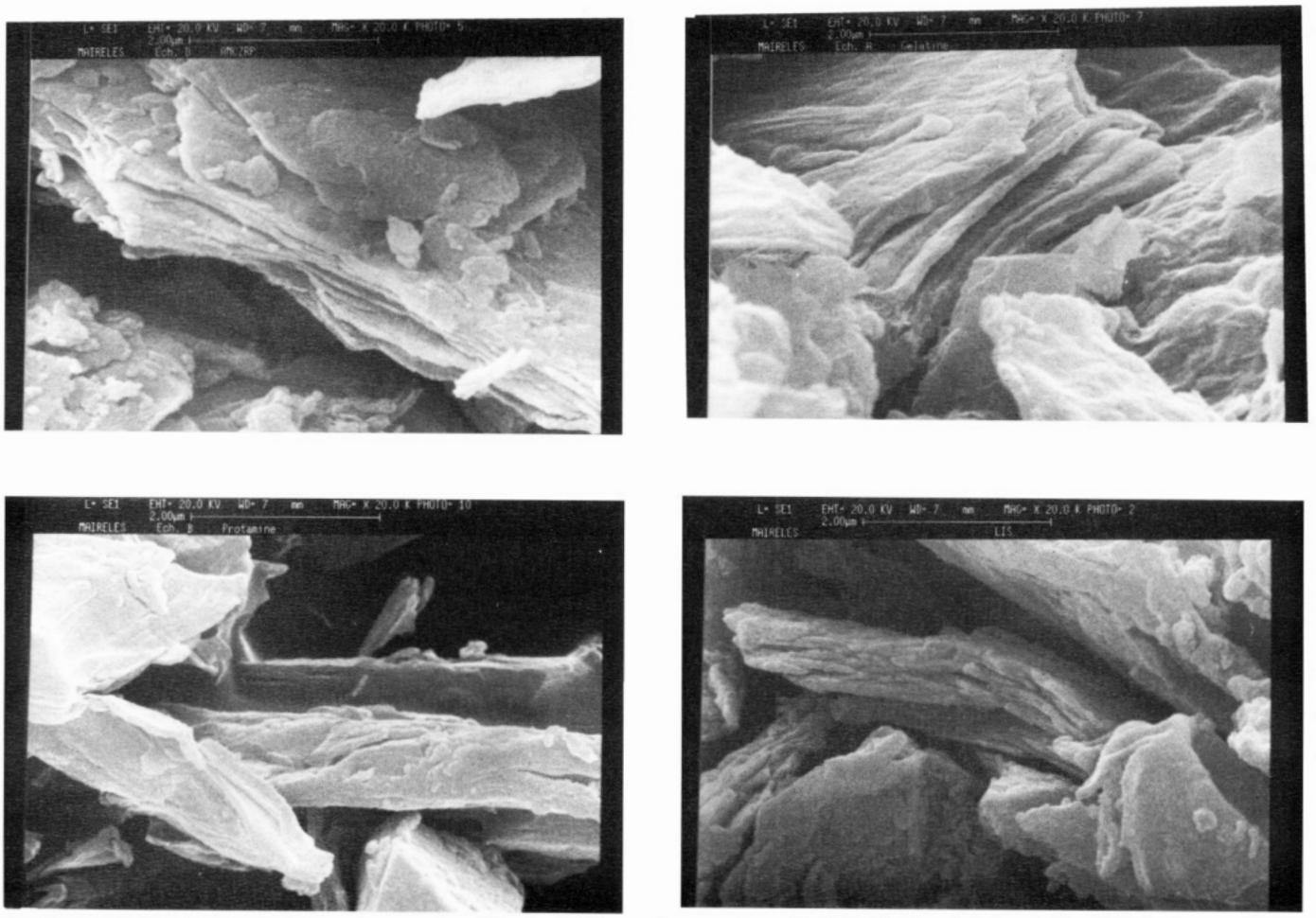

Figure 10. Scanning electron micrographs of (a, top left) ϵ-aminocaproic acid–ZrP; (b, top right) gelatin–ZrP; (c, bottom left) protamine–ZrP, and (d, bottom right) lysozyme–ZrP.

It has previously been concluded from work on clays that whereas both low molecular weight proteins of minimal structural complexity and globular, high molecular weight proteins can be sorbed or exchanged, high molecular proteins of high degree of crystalline order, and which cannot be modified without destruction of the primary protein structure, are excluded.[38] Lagaly has also described models for protein adsorption on to clays but considered higher molecular weight polymers such as albumen and lysozyme to be only anchored in the interlayer zone and largely adsorbed on the external surfaces.[41]

Visual evidence for complete inclusion of the protein is provided by scanning electron microscopy (Figure 10), where the platelets of zirconium phosphate may be seen in each case. Importantly, single phase materials were always observed, and no heterogeneity could be distinguished within the samples. No significant reduction in particle size is detected on the exchange of gelatin or lysozyme with aminocaproic acid; however, a relative reduction in dimension of the phosphate platelets may be discerned for the protamine–ZrP intercalate. Protamine creates a solution of basic pH due to the high percentage of basic amino acids (predominantly arginine) in its composition, which causes, with time, a certain degree of hydrolysis of the phosphate layers.

(40) Albertsson, J.; Oskarsson, A.; Tellgren, R.; Thomas, J. O. *J. Phys. Chem.* **1977**, *81*, 1574.
(41) Perez-Rodriguez, J. L.; Weiss, A.; Lagaly, G. *Clays Clay Miner.* **1977**, *25*, 243.

Table 3. IR Spectra of Biopolymer–α-ZrP Nanocomposites: Amide Group Absorption

sample	amide I ν(C=O)	amide II δ(N–H)	amide A Fermi resonance	amide B ν(N–H)
gelatin	1666	1535, 1553	≈3300 vb	3083
gelatin–ZrP	1660	1544	3325	3078
protamine	1658	1536	3305 vb	3069
protamine–ZrP	1662	1542	3287	3081
lysozyme	1658	1529	3303 b	3059, 3076
lysozyme–ZrP	1657	1540	3287	3088

Table 3 summarizes the values of characteristic IR vibrations of the amide groups of bulk and intercalated biomolecules. The disappearance of the spectral signature of ϵ-aminocaproic acid clearly shows it to have been displaced from the interlayer region by the new guests. Amide I and II modes occur in the ranges 1657–1666 cm^{-1} and 1536–1554 cm^{-1}, respectively. Changes in position and intensity of intercalated molecules compared with those of the corresponding protein ex situ demonstrates interaction with the layer to be different from that present between polypeptide chains in the bulk biopolymer.

Formation of Nylon Nanocomposites. When thermogravimetric analysis of the ϵ-aminocaproic acid intercalate is performed under nitrogen, a plateau in the weight loss curve is clearly observable at 260–270 °C, when two endothermic events are seen in DTA centered at 242 and 278 °C (Figure 3). The XRD pattern of the material recovered at this point indicates the layer structure of the precursor to be retained, but with loss

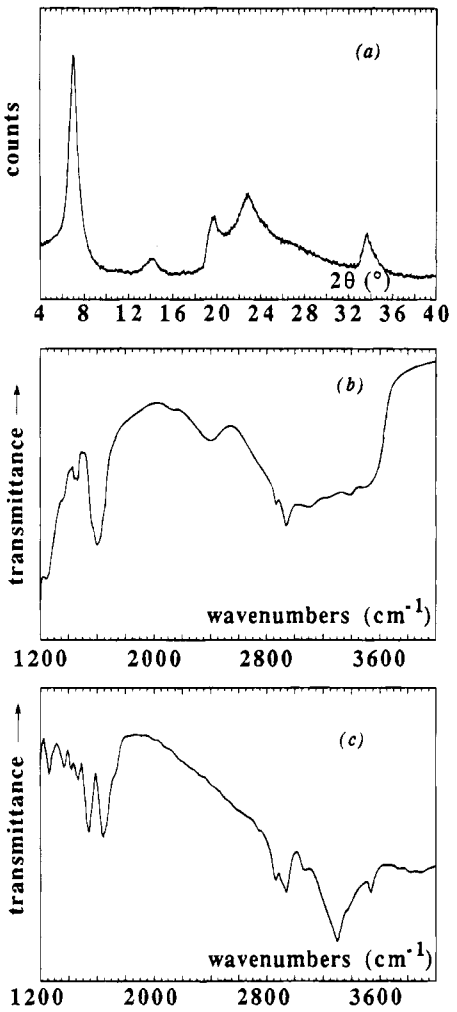

Figure 11. (a) Powder X-ray diffraction patterns of nylon–ZrP, (b) infrared spectrum of nylon–ZrP, and (c) infrared spectrum of nylon recovered from the composite by HF destruction of the phosphate matrix.

of organic matter (11% from TGA) and reorientation, since the basal spacing decreases to 12.2 Å (Figure 11a). The thermogram shows that this composite, of composition $\{\alpha\text{-}Zr(HPO)_4)_2(-HN(CH_2)_5CO-)_{0.5}$, exists over the temperature range 270–300 °C, followed by a progressive degradation and elimination of organic matter up to 900 °C.

Calcination of aminocaproic acid–metal ion-exchange clay intercalates under similar conditions is reported to lead to the formation of nylon-6 through condensation of protonated $-NH_3$ with CO_2H groups,[28] and it is concluded that a similar reaction occurs in α-ZrP, where the head-by-tail disposition of the aminocaproic acid monomers organized by the host matrix is conducive to polyamide formation. Evidence for in situ polymerization comes from DTA where, in contrast to the bulk polymer, which shows a melting transition at 229 °C, the ZrP–nylon nanocomposite (recovered at 278 °C and resubmitted to thermal analysis) shows no thermal events over the range 80–320 °C. This difference in behavior between bulk and confined polymers has been attributed to inhibited formation of polymer crystallites within a spacially restricted environment of a layered matrix.[19,20]

Formation of polymer chains or networks within the confines of a host matrix goes beyond the energetic requirement of intercalation or ion-exchange processes of monomeric species driven by proton or electron transfer, differences in hydration energy, etc.; structural factors beyond steric considerations come into play, and a certain degree of commensurability of the structures of host and polymerized guest might be expected to favor the polymerization process. In the course of the polycondensation process the amino acid chains must change their relative orientation, such that the difference between the translational period of the monomer and the polymer approaches zero,[16] and conditions appropriate for topochemical polymerization are united. With the partial deintercalation that takes place at ca. 250 °C (formation of the 10.6 Å AMC–α-ZrP phase), the remaining amino acid is no longer forced to adopt a slanted position and can rearrange to something closer to a layer-parallel monolayer, the axis of which will still lie such as to maximize hydrogen-bonding interactions with the layers. It has previously been suggested, based on the similarity between the length of amino acid molecules and the unit-cell dimension along the *a* axis, on packing considerations and host–guest interactions,[25] that amino acids such as lysine lie with their long axes parallel to the **a** direction of α-ZrP at low uptake. Aminocaproic acid has a molecular dimension similar to lysine and, although there is no direct X-ray evidence, it is possible that, in the present case, ϵ-aminocaproic acid is also oriented parallel to the direction of the *a* axis in the zirconium phosphate structure.

At the polymerization temperature (278 °C), the aminoacid molecules are favorably disposed for the condensation reaction, the interchain hydrogen bonds are broken and water is split out, leaving the amide linkage $-C(=O)NH-$. The mechanism of polymerization of the monomer is identical to that which occurs in the bulk, where individual polymer chains are derived from aminocaproic acid molecules lying within one layer of the crystal.[42]

The necessity for orientation of the aminocaproic acid molecules in the interlayer region into an arrangement favourable for condensation polymerization is the factor decisive in determining the stoichiometry of the nylon-6–α-ZrP nanocomposite. From unit-cell dimensions of the aminocaproic acid crystal, it may be estimated that the aminocaproic acid molecule occupies a volume of approximately 190 Å^3. Compared with the volume available per intercalated molecule under conditions of the observed free height in the dehydrated AMC–α-ZrP phase, up to 1.1 molecules of AMC could be incorporated; in different preparations, the oberved stoichiometry varied between 0.8 and 0.9. As described above, at higher temperatures, aminocaproic acid is progressively eliminated, until at ca. 250 °C, spontaneous reorientation occurs to give the layer-parallel phase. In such a disposition, the covering effect is much higher, and the limiting stoichiometry for this phase, based on geometrical considerations, is only 0.5 mol of AMC/mol of α-ZrP. The stoichiometry attained at this point by the system obviously determines the maximum quantity of organic matter present in the nylon–α-ZrP composite formed subsequently. Thus, whereas a stoichiometry in this system as high as 0.86 nylon-6/α-ZrP can be calculated based on free volume and the geometry of

(42) Bodor, G.; Bednowitz, A. L.; Post, B. *Acta Crystallogr.* **1967**, *23*, 482.

the nylon-6 unit,[43] the experimentally observed stoichiometry is $\{\alpha\text{-}Zr(HPO_4)_2(-HN(CH_2)_5CO-)_{0.5}$, i.e., the same ratio of organic–inorganic matter as in its immediate precursor.

When nylon-6 is formed from ϵ-aminocaproic acid in the bulk, crystalline material can be obtained under appropriate conditions of temperature and pressure. The polymer chains in this highly crystalline nylon-6 are interlinked to give an oriented, layered arrangement, the distance between layers being ca. 4.8 Å, the repeat distance along the polymer chain being 8.6 Å, and the distance between chains in the same layer ca. 4.0 Å.[42] It is interesting to compare these values with those that can be deduced for the polymer nanocomposite from the above structural model. The free height available for the polymer in the 12.2 Å nylon–ZrP phase is 12.2 − 6.6 = 5.6, adequate for inclusion of a single chain of nylon-6 between the phosphate layers (cf. interlayer distance in nylon-6 of 4.8 Å).

Of clear importance is the characterisation of the occluded nylon polymer, in particular with respect to its interaction with the layer and its structure. The IR spectrum of the compound formed after calcination at 270 °C (Figure 11b) is markedly different from that of its precursor (Figure 5), with disappearance of the absorption bands characteristic of $-NH_3^+$ groups, and a modification in the 1550–1700 cm^{-1} range which is interpreted in terms of the replacement of carboxylic acid C=O group vibrations by amide I [ν(C=O)] and amide II [(δ(N–H), ν(C–N)] bands at 1602 and 1547 cm^{-1}, respectively, together with those at 3236 (amide A) and 3104 (amide B) cm^{-1}.

Treatment of the nylon nanocomposite with an aqueous solution of HF destroys the inorganic component and liberates nylon, which can then be studied by various techniques. The IR spectrum of this HF-extracted nylon is well-resolved, presenting amide (I and II) bands at 1640 and 1547 cm^{-1}, respectively, in complete agreement with the positions of those exhibited by crystalline nylon 6 (1640 and 1546 cm^{-1})[44] (Figure 11c). It can be concluded, from the positions of the amide absorptions in the free and occluded polymer, that strong interaction of inserted nylon with the layers, via C=O and N–H groups occurs. This is supported by abortive attempts to extract nylon by use of *m*-cresol at reflux temperature, in sharp contrast to the facile extraction of nylon from montmorillonite analogues.

The ^{13}C CP MAS NMR spectra of ϵ-aminocaproic acid, AMC–α-ZrP, nylon–ZrP intercalates, and nylon prepared ex situ reproduced in Figure 12 demonstrate the expected evolution from bulk to intercalated ϵ-aminocaproic acid. Theoretical calculations by using the "additive shift technique"[45] allows the observed resonances to be assigned (Table 4). In the bulk, ϵ-aminocaproic acid exists in the zwitterionic form, each ion forming three N–H–O hydrogen bonds with adjacent ions to form a double-layered structure, with the two C–O bonds of the carboxylate group almost equal in length.[42] In ^{13}C NMR, this structural arrangement is manifested by observed chemical shifts for C1 (39.1 ppm) and C5 (40.5 ppm), relative to TMS (numbering scheme $HO(O)C-C1-C2-C3-C4-C5-NH_2$ in monomeric aminocaproic acid; $-(O)C-C1-C2-C3-C4-C5-NH-$ in the corresponding polymer), which are close to those calculated for carbon atoms bonded to COO^- and NH_3^+ groups, being 38.8 and 40.8 ppm, respectively.

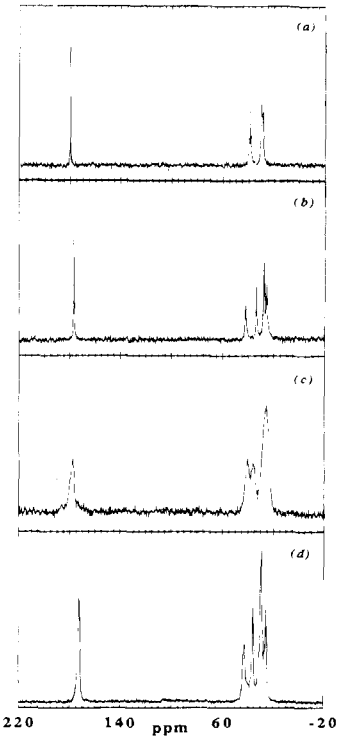

Figure 12. ^{13}C CP MAS NMR spectra of (a) bulk ϵ-aminocaproic acid, (b) α-AMC–ZrP, (c) nylon–ZrP intercalates, and (d) nylon prepared ex situ.

Table 4. ^{13}C CP-MAS NMR Chemical Shifts[a] of Bulk ϵ-Aminocaproic Acid, the ϵ-Aminocaproic Acid–ZrP Intercalate, and Corresponding Nylon–ZrP Nanocomposite and Nylon Prepared ex Situ from ϵ-Aminocaproic Acid

	C=O[b]	C1	C2	C3	C4	C5
ϵ-aminocaproic acid	182.0	39.1	29.6	29.6	31.1	40.5
ϵ-aminocaproic acid–ZrP	178.1	34.1	25.9	28.2	28.2	42.7
nylon–ZrP	179.2	37.5	26.7	26.7	26.7	41.3
nylon ex situ	173.3	36.5	26.2	30.1	30.1	43.3

[a] TMS as reference. [b] Numbering: $HO(O)C-C1-C2-C3-C4-C5-NH_2$ in monomeric aminocaproic acid; $-(O)C-C1-C2-C3-C4-C5-NH-$ in the corresponding polymer.

On intercalation of aminocaproic acid, the resonances at 178.1 ppm for C–O and 34.1 ppm for C1 confirm the regeneration of carboxylic acid group, and the downfield shift of C5 (42.7 ppm) points to an interaction of NH_3^+ groups with the layers weaker than that between ions in bulk ϵ-aminocaproic acid. As previously reported by Hagen et al.[46] in a comparative study of aliphatic carboxylic acid and carboxylate anions, rationalization of the observed and calculated evolution of the shielding of α-carbon atoms in terms only of the electronegativity of the substituent is difficult, the introduction of second-order paramagnetic effect on carbon resonances being required. The carboxylate group is expected to be substantially less electronegative than the carboxylic acid group, and the calculated value for the carboxylic

(43) Holmes, D. R.; Bunn, C. W.; Smith, D. J. *Polym. Sci.* **1955**, *17*, 159.
(44) Pouchert, C. J. *Aldrich Library of FT-IR Spectra*; Aldrich Chemical Co. Inc.: Milwaukee, WI, 1985; Vol. 2, p 1198.
(45) Grant, D. M.; Paul, E. G. *J. Am. Chem. Soc.* **1964**, *86*, 2984.
(46) Hagen, R.; Roberts, J. D. *J. Am. Chem. Soc.* **1969**, *91*, 4504.

acid group of 34.8 ppm represents an upfield shift, exactly the opposite of what is measured experimentally.

After calcination, intercalated aminocaproic acid molecules reorientate and polymerize to form nylon-6 in the interlayer region of zirconium phosphate. By comparing the ^{13}C NMR spectra of inserted nylon and nylon prepared ex situ, some remarks can be made. Higher C1 and C(=O) chemical shifts for inserted than for bulk nylon could be explained on the basis of a strong interaction of carbonyl groups of the polymer with the interlayer P−OH groups which stabilizes nylon-6 at high temperature. The observed upfield chemical shift for C5 of occluded nylon relative to bulk nylon may reflect the formation of hydrogen bonds (C=O−H−N) between adjacent chains in the latter, which causes a decrease in the screening effect on C5. Conversely, interaction between NH and POH groups is less effective, probably because of steric and packing considerations.

Acknowledgment. P.M.-T. thanks the European Commission for the award of a fellowship through the Brite-EuRam II programme of the European Commission, Contract ERB BRE2-CT93-3005. This work was partially supported by the European Commission under Brite-EuRam Contract BRE2-CT93-0535. Y.D. is grateful to the CNRS for the award of a postdoctoral fellowship.

CM940465M